Enzyme Substrates

DOI: 10.1002/ange.201402000

Substrate Profiling of Glutathione S-transferase with Engineered Enzymes and Matched Glutathione Analogues**

*Shan Feng, Lei Zhang, Gulishana Adilijiang, Jieyuan Liu, Minkui Luo, and Haiteng Deng**

Abstract: *The identification of specific substrates of glutathione S-transferases (GSTs) is important for understanding drug metabolism. A method termed bioorthogonal identification of GST substrates (BIGS) was developed, in which a reduced glutathione (GSH) analogue was developed for recognition by a rationally engineered GST to label the substrates of the corresponding native GST. A K44G-W40A-R41A mutant (GST-KWR) of the mu-class glutathione S-transferases GSTM1 was shown to be active with a clickable GSH analogue (GSH-R1) as the cosubstrate. The GSH-R1 conjugation products can react with an azido-based biotin probe for ready enrichment and MS identification. Proof-of-principle studies were carried to detect the products of GSH-R1 conjugation to 1-chloro-2,4-dinitrobenzene (CDNB) and dopamine quinone. The BIGS technology was then used to identify GSTM1 substrates in the Chinese herbal medicine Ganmaocongji.*

Glutathione S-transferases (GSTs; EC 2.5.1.18) are the major phase II metabolic enzymes and they reversibly catalyze the conjugation of the reduced form of glutathione (GSH) to a wide range of xenobiotic substrates and endogenous metabolites.[1–3] GSTs are widely distributed in both prokaryotes and eukaryotes and play important roles in cellular detoxification and drug metabolism. The GST family consists of at least four subgroups: cytosolic GSTs (cGSTs), mitochondrial GSTs (kappa GSTs), microsomal GSTs (MAPEG), and bacterial fosfomycin-resistance proteins. cGSTs are subdivided into thirteen subclasses, including alpha/mu/pi, theta, omega, sigma, and zata, based on their structural and chemical properties.[4–6] Over the last decade, it has been realized that GSTs play important roles in physiological and pathological processes.[7–10] The catalytic mechanisms and physiological roles of GSTs have been well established,[11,12] but how GSTs recognize their specific substrates during the process of phase II metabolism remains to be elucidated. Identification of the specific set of substrates of a designated GST is crucial for understanding phase II drug metabolism, especially for drugs containing complex mixtures such as Chinese herbal medicines extracted from plants.

The field of substrate profiling has seen intensive investigation of important enzyme classes that act on protein substrates, including kinases, proteases, methyltransferases, and acetyltransferases. Pioneering work by Shokat et al. has led to the development of chemical biology methods for the identification of kinase substrates.[13,14] Recently, Luo et al. developed a technology termed bioorthogonal profiling of protein methylation (BPPM) to profile the substrates of specific methyltransferases.[15] As the most recent example, Zheng et al. implemented a protein engineering approach together with acetyl-CoA analogues to profile the substrates of designated acetyltransferases.[16] However, the previous examples with engineered proteins and matched cosubstrate analogues have mainly focused on enzymes that have broad substrate specificity for particular biological macromolecules such as DNA, RNA, and proteins. Little effort has been made to apply the protein-engineering approach to enzymes that have broad substrate specificity for small molecules, which can be more difficult to characterize given their low molecule weights. Herein, we report a method termed *b*ioorthogonal *i*dentification of *G*ST *s*ubstrates (BIGS) for profiling the substrates of a specific GST. In BIGS, alkyne-containing GSH analogues are synthesized and used as cosubstrates for an engineered mu-class GST (GSTM1). As illustrated in Scheme 1, the engineered GST catalyzes the conjugation of a GSH analogue and a substrate to generate a glutathionylated product that further reacts with an azido-biotin reagent; the biotin-containing products are then enriched by using streptavidin beads before characterization of the products by mass spectrometry.

GSH analogues were synthesized with the incorporation of a terminal alkyne group (Scheme 1; butyl alkynyl ester GSH and proparagyl amide GSH, denoted as GSH-R1 and GSH-R2, respectively). By using 1-chloro-2,4-dinitrobenzene (CDNB) as the model substrate, we showed that wild type (WT) GSTM1 efficiently catalyzes the conjugation of GSH to CDNB, but the conjugation efficiencies are rather low for both GSH-R1 and GSH-R2. In order to increase the conjugation efficiency of GSH-R1 or GSH-R2 with CDNB, genetic engineering of GSTM1 was carried out with the guidance of the crystal structure of a GSTM1–GSH complex (Figure 1).

The residues W40, R41, and K44 in GSTM1 are located near the C-terminal carboxyl group of GSH and weakly interact with the negatively charged oxygen atoms of GSH.

[*] Dr. S. Feng, L. Zhang, G. Adilijiang, J. Liu, Prof. H. Deng
MOE Key Laboratory of Bioinformatics, School of Life Sciences
Renhuan Building 301, Tsinghua University, 100084 Beijing (China)
E-mail: dht@mail.tsinghua.edu.cn

Prof. M. Luo
Molecular Pharmacology and Chemistry Program
Memorial Sloan-Kettering Cancer Center
New York, 10065 NY (USA)

[**] This work was supported in part by the Center for Life Sciences (Tsinghua University), the National Natural Science Foundation of China (No. 31270871), and Department of Education China (No. 2012Z02293) and the Global Science Alliance Program of ThermoFisher Scientific.

Supporting information for this article is available on the WWW under http://dx.doi.org/10.1002/anie.201402000.

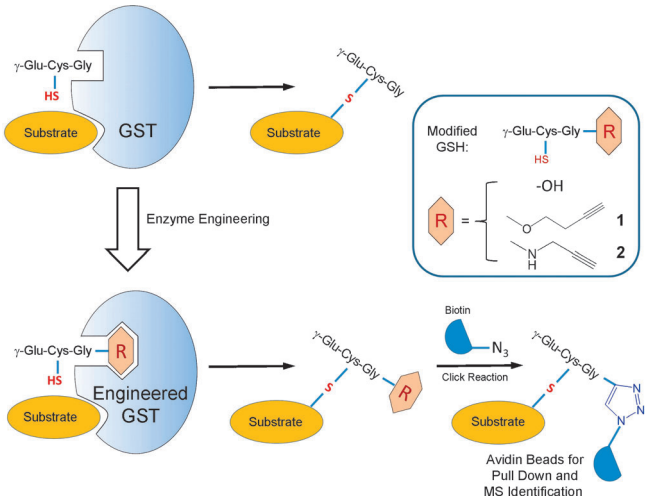

Scheme 1. Scheme of BIGS. An engineered GST combined with clickable GSH analogues is used to label GST substrates. The C-terminal GSH binding sites of the GST are rationally modified to accommodate the alkyne group of the GSH analogues. This product can further react with an azido-based probe through a click reaction for substrate labeling and MS analysis.

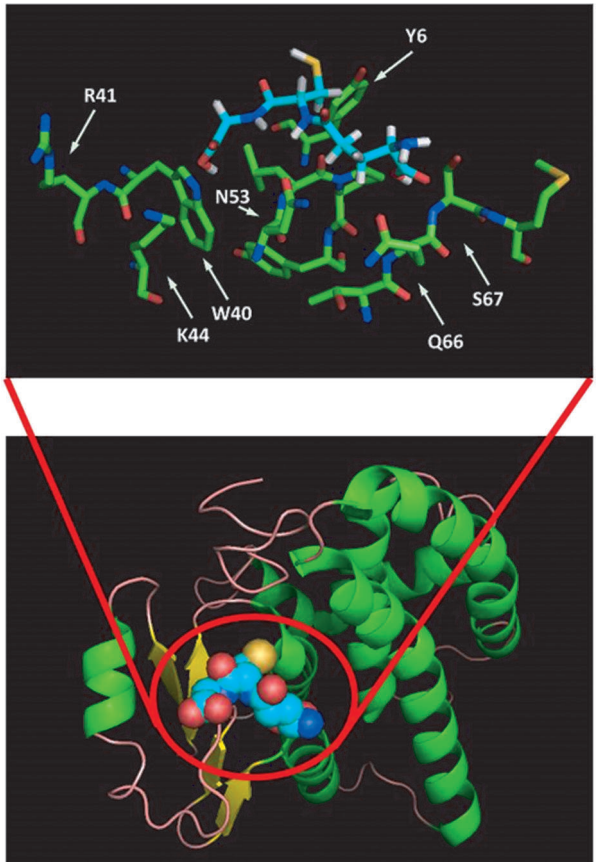

Figure 1. The monomeric structure of the mu-class GST GSTM1 from *Schistosoma japonicum* and a ball-and-stick model of the docking sites of GSH in the binding pocket of GSTM1 (from PDB 1UA5). The amino acid residues that interact with GSH are indicated by white arrows.

Mutations to these remote residues may not affect the conjugation of the sulfur atom of the GSH analogues to the substrate but could generate a spacious vacant pocket to accommodate the bulky alkynyl group of R1 and R2. We generated twelve GSTM1 mutants, some of which exhibit decreased binding affinity for GSH (Figure S1 in the Supporting Information). Although the low affinity of these mutants makes their purification by glutathione–Sepharose Column difficult, this observation is consistent with their decreased binding affinity for GSH.

In contrast to the loss of affinity for GSH of some of the GSTM1 mutants, the activities of certain GSTM1 mutants towards GSH analogues were significantly enhanced. As shown in Table 1, the W40 GSTM1 mutants generally show lower glutathionylation activity than those carrying R41 or

Table 1: Relative enzymatic activities of WT GSTM1 and the twelve mutants on the model substrate CDNB, with GSH and GSH analogues (R1 & R2) as cosubstrates.[a]

GSH Analogues	GSH	R1	R2
	–OH	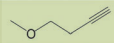	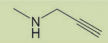
No Enzyme	11.3%	12.2%	8.2%
WT	98.8%	23.3%	30.2%
K44G	97%	39.5%	25%
K44A	95.9%	44.4%	36.9%
K44S	95.6%	47%	35.6%
W40G	81.1%	36.9%	10.4%
W40A	89.7%	37.3%	14.6%
W40F	96.7%	49.9%	35.1%
R41A	97.5%	44.5%	**50.8%**
R41H	99.5%	43.6%	**52%**
K44A-W40G	65.7%	56%	24.4%
K44A-W40F	95.2%	64.4%	37.1%
K44G-W40A-R41A	49.3%	**82.7%**	38.5%
K44S-W40F-R41A	66.2%	60.5%	29.5%

[a]The numbers were calculated based on measurement of the consumption of CDNB by HPLC. The enzyme variants that show the highest activities towards GSH-R1 and GSH-R2 are highlighted in red. The measurements of conversion efficiency were performed twice (see the Supporting Information).

K44 mutations, thus suggesting that the former is more crucial to the recognition of GSH as a cosubstrate. By contrast, R41 GSTM1 mutants show decent activity towards GSH-R1 and GSH-R2; and K44 GSTM1 mutants show decent activity towards GSH-R1. In general, GSH-R1 is a more reactive cosubstrate than GSH-R2 in the conjugation with CDNB catalyzed by the engineered GST.

To further boost the selectivity of the engineered GST toward GSH-R1/2 over the native GSH as cosubstrates, we generated double/triple mutants of W40, R41, and K44. The GSTM1 mutant K44G-W40A-R41A shows the lowest activity toward unmodified GSH, but it gains significant activity with GSH-R1 as a cosubstrate (highlighted in red in Table 1). The reaction efficiency of CDNB with GSH-R1 catalyzed by the K44G-W40A-R41A GSTM1 mutant (GST-KWR) is close to 85% with the current assay (Table 1 and Figure S2). This process is enzyme-dependent because a higher concentration

of the enzyme further enhances the conjugation efficiency with CDNB, which is fully converted to its conjugates within 1 h in the presence of 0.1 mg mL^{-1} GST-KWR (Figure S3). Furthermore, we have measured the apparent kinetic parameters of the conjugation reactions catalyzed by WT GSTM1 and GST-KWR and these parameters are listed in Table S1 in the Supporting Information. The K_m-R1 value for GST-KWR (0.22 mM) is four times lower than that for WT GSTM1 (0.91 mM), thus indicating that the K44G-W40A-R41A mutations enhanced the binding affinity between the enzyme and GSH-R1. The k_{cat} value of R1–CDNB conjugation catalyzed by GST-KWR is about 2.04 s^{-1}, which is close to the value for GSH–CDNB conjugation catalyzed by WT GSTM1 (2.28 s^{-1}). These results demonstrate that the combination of GST-KWR and GSH-R1 gives a similar catalytic efficiency to that of WT GSTM1 and GSH.

When CDNB was incubated with a mixture of GSH and GSH-R1 in the presence of WT GSTM1, 95% of the CDNB was converted into the conjugate with GSH (Figure S4B), thus indicating that WT GSTM1 strongly prefers GSH as a cosubstrate. In contrast, when incubated with the mutant enzyme GST-KWR, more than 60% of the CDNB was conjugated with GSH-R1 (Figure S4C). When the concentration of GSH-R1 was increased to 2 mM (2-fold higher than that of GSH), less than 10% of the CDNB conjugation product with GSH was observed (Figure S4D). These competitive experiments demonstrate that GST-KWR prefers GSH-R1 as a cosubstrate. In the presence of excess GSH-R1 as a cosubstrate probe, the GST-KWR variant efficiently catalyzes the conjugation of GSH-R1 with CDNB even in the presence of GSH.

Tandem mass spectrometry (MS/MS) analysis was further carried out to confirm the conjugation product of CDNB with GSH-R1. The monoisotopic peak of the product is observed at m/z 526.12, which corresponds to the dechlorination reaction product (Figure 2A). Two fragments are observed at m/z 399.09 and 397.37, corresponding to the b_2 and y_2 ions of the conjugated product (Figure 2B). The MS/MS spectra of products of CDNB conjugation with GSH or GSH-R2 display a similar fragmentation pattern (Figure S5). The product of the conjugation of GSH-R1 to CDNB was further reacted with a biotin probe (azide–PEG3–biotin) by copper-catalyzed azide–alkyne cycloaddition (CuAAC) followed by isolation with streptavidin beads; the final product was detected by LC–MS at m/z 970.34 (Figure S6), thus indicating that the GST substrate was enriched through the affinity purification.

The major fragment of the biotinylated product was observed at m/z 270.13 and denoted as β (Figure S7). The fragment β was generated from the breakage of the ether bond in the azide–PEG3–biotin reagent (Figure S8B). Other characteristic fragments that are not related to the substrate structure are observed, including y_1,γ, β, b_1-H_2O, and b_1-COOH ions (Figure S7B). The b_1-H_2O and b_1 ions are specific to GSH fragmentation owing to an unusual amide bond formation between a glutamic acid residue and a cysteine residue. These fragments observed in the MS/MS spectra of the azide–PEG3–biotin labeled products are summarized in Figure 3 and the fragment β can assist in the detection of GST substrates.

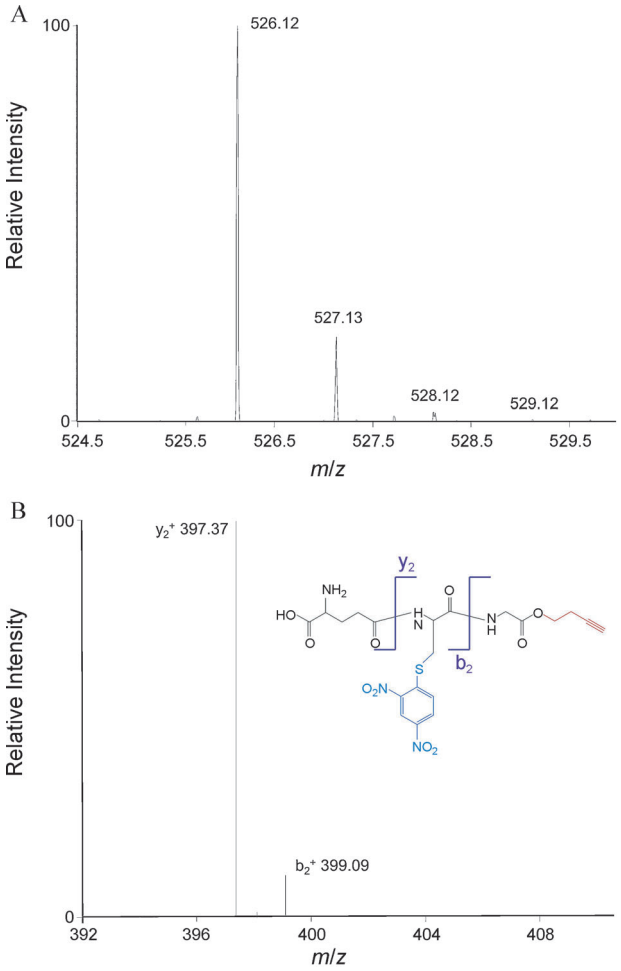

Figure 2. Mass spectrometry analysis of the product from the reaction of CDNB and GSH-R1. A) An MS spectrum of the product; the monoisotopic peak is at m/z 526.12. B) An MS/MS spectrum of the product. The peaks at m/z 397.37 and 399.09 correspond to the y_2 and b_2 ions.

To further demonstrate the utility of the GST-KWR variant and its matched GSH-R1 cosubstrate, we investigated whether the enzyme–cosubstrate pair can label GST substrates through other mechanisms. In comparison to CDNB, which is labelled through GST-catalyzed aromatic nucleophilic substitution, the neurotransmitter dopamine is a GST substrate that is labelled through nucleophilic addition. During Phase I metabolism, the hydroxy group of dopamine is oxidized into the quinone form, which is then modified with GSH.[17–18] After oxidizing dopamine with tyrosinase, the mixture was incubated with GSH-R1 in the presence of liver microsomes and GST-KWR. After a click reaction with the biotinylated reagent, the final products were enriched by using streptavidin beads and analyzed by LC–MS (Figure S9). The final product was identified at m/z 955.49 and its major fragments β, b_1*-H_2O, b_1*-COOH ions were observed in the MS/MS spectrum, thus indicating that GST-KWR efficiently catalyzes the addition of GSH-R1 to the quinone moiety.

We then explored the applicability of this method to the profiling of substrates of GSTM1 in a complex sample. The Chinese herbal medicine Ganmaochongji is a widely used

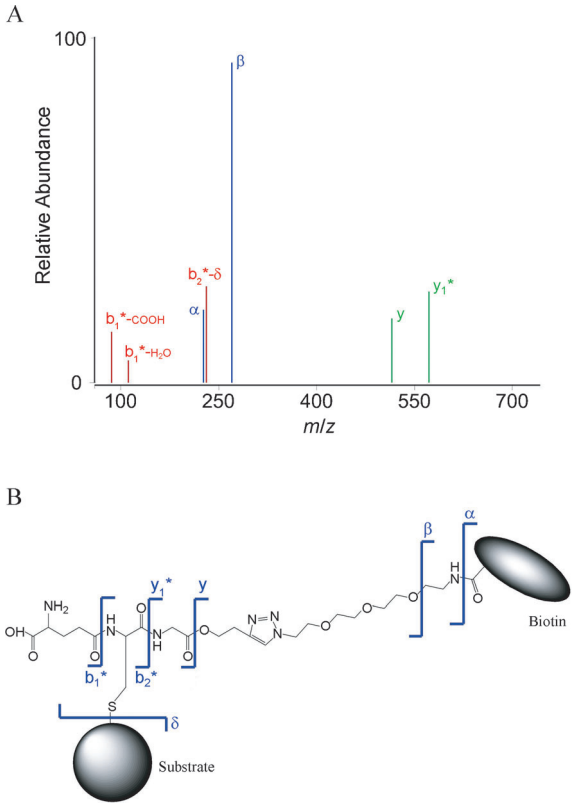

Figure 3. A characteristic MS/MS spectrum of the detected products from fragmentation of the biotinylated GSH-R1–substrate conjugates. A) Seven peaks can be identified: b_1*-COOH, b_1*-H_2O, α, b_2*-δ, β, γ and y_1*. B) The structure and fragmentation pattern of the detected molecules, which are the conjugated products of the substrates with GSH-R1 and azide–PEG3–biotin.

plant extract mixture used to suppress the symptoms of colds and flu, and it is comprised of extracts from more than ten different herbs, including throrowax root, bitter almond, *Schizonepeta*, and mint. Ganmaochongji was dissolved in boiling PBS (pH 7.0) and mixed with liver microsomes and reacted with the clickable probe GSH-R1 (with unmodified GSH as the negative control) in the presence of GST-KWR. The products were conjugated with biotin and enriched by using streptavidin beads, followed by LC–MS/MS analysis. Based on the two mechanisms leading to conjugation of a substrate with GSH, substitution or nucleophilic addition, the reaction products are classified as arising from dehalogenation, quinone addition, or ring opening of epoxides. For nucleophilic additions such as the quinone addition and the ring opening of epoxides, the *m*/*z* values for the predicted products are expected to be 803.33 higher than those of the original molecules owing to the addition of GSH-R1 and the azide–PEG3–biotin probe. In dechlorination or debromination, the masses of the products are either 767.35 or 731.37 higher than that of the original molecule owing to addition of the probe(s) and loss of the halogen atom(s). Based on these characteristic mass changes, we identified a set of mass shifts that are consistent with the conjugation products by searching the METLIN database with 5 ppm mass accuracy.[19] Several potential GSTM1 substrates were identified (Figure S10), including cyclodopaglucoside, which is the intermediate in betaltian biosynthesis and is present in *Perillafrutescens*, a component of Ganmaochongji. Also found was a product of the dechlorination of 7-chloro-6-demethylcepharadione B, which is an aporphine-related alkaloid from *Houttuyniacordata* that is used as a bioactive component against colds.[20] Another potential substrate is callystatin A, which belongs to the leptomycin family of antibiotics and was characterized from the marine sponge *Callyspongia truncate*.[21] Callystatin A was identified recently in plants such as *Coleus forskohlii*. Our results indicate that callystatin A could be one of the active substrates of GSTM1 in Ganmaochongji. Other potential GSTM1 substrates with characteristic fragmentation patterns in MS/MS spectra are summarized in Table S2 in the Supporting Information. It is worth mentioning that most of the above-described products were not observed in the reaction mixture without the GST-KWR enzyme, except for two products observed at *m*/*z* 1161.44 and 1260.65. However, the intensities of these two products were 215 and 8 times higher in the presence of GST-KWR under identical conditions (Figure S11,12 and Table S2). These results demonstrated that the above-described products were generated through reactions catalyzed by GST-KWR.

In summary, we have developed a new clickable GSH analogue, GSH-R1, which forms conjugates with GST substrates in reactions catalyzed by the engineered enzyme GST-KWR. Following biotinylation, the conjugation products can be readily enriched and display characteristic fragments in MS/MS spectra for further characterization. More importantly, these characteristic fragments can be used to dissect the signals even in the context of complex mixtures and can be coupled with isotopic dilution mass spectrometry for further characterization if an isotopic GSH-R1 probe is used. By using CDNB, dopamine, and the Ganmaochongji mixture as substrates, we demonstrated the robustness of this method for labeling GST substrates. This method therefore demonstrates potential for profiling GST substrates in complex mixtures.

Received: February 1, 2014
Revised: March 30, 2014
Published online: May 30, 2014

Keywords: click chemistry · glutathione S-transferases · mass spectrometry · protein engineering · substrate profiling

[1] J. Booth, E. Boyland, P. Sims, *Biochem. J.* **1961**, *79*, 516.
[2] B. Combes, G. S. Stakelum, *J. Clin. Invest.* **1961**, *40*, 981.
[3] T. D. Boyer, *Hepatology* **1989**, *9*, 486.
[4] B. Mannervik, P. G. Board, J. D. Hayes, I. Listowsky, W. R. Pearson, *Methods Enzymol.* **2005**, *401*, 1.
[5] J. D. Hayes, J. U. Flanagan, I. R. Jowsey, *Annu. Rev. Pharmacol. Toxicol.* **2005**, *45*, 51.
[6] C. B. Pickett, A. Y. Lu, *Annu. Rev. Biochem.* **1989**, *58*, 743.
[7] K. D. Tew, Y. Manevich, C. Grek, Y. Xiong, J. Uys, D. M. Townsend, *Free Radical Biol. Med.* **2011**, *51*, 299.
[8] E. Laborde, *Cell Death Differ.* **2010**, *17*, 1373.
[9] P. G. Board, D. Menon, *Biochim. Biophys. Acta Gen. Subj.* **2013**, *1830*, 3267.
[10] H. Raza, *FEBS J.* **2011**, *278*, 4243.
[11] R. N. Armstrong, *Chem. Res. Toxicol.* **1997**, *10*, 2.

[12] D. Sheehan, G. Meade, V. M. Foley, C. A. Dowd, *Biochem. J.* **2001**, *360*, 1.
[13] D. J. Maly, J. A. Allen, K. M. Shokat, *J. Am. Chem. Soc.* **2004**, *126*, 9160.
[14] J. J. Allen, S. E. Lazerwith, K. M. Shokat, *J. Am. Chem. Soc.* **2005**, *127*, 5288.
[15] R. Wang, W. Zheng, H. Yu, H. Deng, M. Luo, *J. Am. Chem. Soc.* **2011**, *133*, 7648.
[16] C. Yang, J. Mi, Y. Feng, L. Ngo, T. Gao, L. Yan, Y. Zheng, *J. Am. Chem. Soc.* **2013**, *135*, 7791.
[17] J. Segura-Aguilar, C. Lind, *Chem.-Biol. Interact.* **1989**, *72*, 309.
[18] J. Segura-Aguilar, V. Cortés-Vizcaino, A. Llombart-Bosch, L. Ernster, E. Monsalve, F. J. Romero, *Carcinogenesis* **1990**, *11*, 1727.
[19] T. R. Sana, J. C. Roark, X. Li, K. Waddell, S. M. Fischer, *J. BiomolTech.* **2008**, *19*, 258.
[20] T. T. Jong, M. Y. Jean, *J. Chin. Chem. Soc.* **1993**, *40*, 301.
[21] M. Kobayashi, K. Higuchi, N. Murakami, H. Tajima, S. Aoki, *Tetrahedron Lett.* **1997**, *38*, 2859.

